

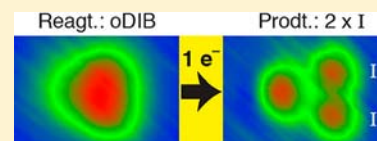
Single-Electron Induces Double-Reaction by Charge Delocalization

Kai Huang,[†] Lydie Leung, Tingbin Lim, Zhanyu Ning, and John C. Polanyi*

Lash Miller Chemical Laboratories, Department of Chemistry and Institute of Optical Sciences, University of Toronto, 80 St. George Street, Toronto, Ontario, M5S 3H6 Canada

W Web-Enhanced Feature S Supporting Information

ABSTRACT: Injecting an electron by scanning tunneling microscope into a molecule physisorbed at a surface can induce dissociative reaction of one adsorbate bond. Here we show experimentally that a single low-energy electron incident on ortho-diiodobenzene physisorbed on Cu(110) preferentially induces reaction of both of the C–I bonds in the adsorbate, with an order-of-magnitude greater efficiency than for comparable cases of single bond breaking. A two-electronic-state model was used to follow the dynamics, first on an anionic potential-energy surface (pes*) and subsequently on the ground state pes. The model led to the conclusion that the two-bond reaction was due to the delocalization of added charge between adjacent halogen-atoms of ortho-diiodobenzene through overlapping antibonding orbitals, in contrast to the cases of para-dihalobenzenes, studied earlier, for which electron-induced reaction severed exclusively a single carbon–halogen bond. The finding that charge delocalization within a single molecule can readily cause concerted two-bond breaking suggests the more general possibility of intra- and also intermolecular charge delocalization resulting in multisite reaction. Intermolecular charge delocalization has recently been proposed by this laboratory to account for reaction in physisorbed molecular chains (Ning, Z.; Polanyi, J. C. *Angew. Chem., Int. Ed.* **2013**, *52*, 320–324).



INTRODUCTION

Electron transfer is fundamental to a wide range of chemistry and photochemistry and is of heightened interest today as a vehicle for solar energy conversion. Here we show multiple bond excitation in single-electron transfer; a low-energy electron of selected energy (1 eV) when transferred from a scanning tunneling microscope (STM) tip to ortho-diiodobenzene results in the efficient concerted breaking of two C–I bonds. This experimental finding is in contrast to previous studies in which a single electron incident on adsorbates at semiconductors^{1,2} and metals^{2–4} has invariably been found to break a single bond in the impacted molecule. Additionally the present study employs *ab initio* theory to identify the multiple bond-breaking as being due to electron charge delocalization within the acceptor molecule. In a recent theoretical study,⁵ we propose that this single-electron charge delocalization can extend along a row of adjacent physisorbed molecules with resultant multibond breaking along the row, as observed experimentally by Maksymovych, Yates and co-workers⁶ but not explained heretofore. In both the intermolecular and the intramolecular⁵ charge flow, the requirement for delocalization is thought to be the observed presence of spatial overlap between adjacent antibonding molecular orbitals into which the added electron is placed.

METHODS

STM Experiments. All experiments were performed in a low-temperature ultrahigh vacuum STM (Omicron), with base pressure $<3.0 \times 10^{-11}$ mbar. STM images were recorded in constant current mode at 4.6 K. The Cu substrate was cleaned by repeated cycles of Ar⁺ bombardment (0.6 keV, 7 μ A) followed by annealing at 800 K, until no contamination could be detected by STM. ortho-Diiodobenzene,

ortho-DIB, (Sigma Aldrich, 99%) was purified by 7 freeze–pump–thaw cycles before use in the experiment and dosed from a capillary tube directed at the copper crystal. The crystal reached a maximum temperature of 8.3 K during dosing. Dissociation of ortho-DIB was electron-induced by placing the STM tip over the middle of the ortho-DIB feature and maintaining a constant bias voltage, +1.10 V, with the feedback loop disabled, for up to 1 s. Product positions with respect to the position of the physisorbed reagent were measured using WSxM.⁷

The electron order for the breaking of both C–I bonds was determined by varying the tunneling current at near threshold voltage of +1.10 V and obtaining the lifetime of a physisorbed ortho-DIB under each pulse current (I) condition. The individual observed times required for reaction were then binned and fitted to an exponential decay function, which yielded the characteristic lifetime, τ , of the ortho-DIB molecule. The reciprocal of τ was the rate of reaction, R , for each particular I value. These values were used to obtain the log R vs log I plot in Figure 2b. The errors presented for each log R value are derived from the uncertainty of the fit for the lifetime. In fitting the order of reaction, n , in Figure 2b, each data point was also weighted using the error in log R .

Theory. Density function theory (DFT), molecular dynamics (MD) and STM image simulation methods for this study have been detailed in previous publications.^{5,8,9} Simulations were obtained using the Vienna Ab-initio Simulation Package (VASP),¹⁰ including a semiempirical van der Waals' correction.¹¹ The surface Brillouin zones were sampled using the gamma point only. Electronic structures were calculated through a generalized gradient approximation using the Perdew–Burke–Ernzerhof functional¹² with projector augmented waves. The supercell (6×6) consisted of 180 copper atoms in five layers, and a vacuum gap of at least 15 Å. The STM image simulations were generated by bSKAN¹³ using the calculated wave functions of the initial and final states from VASP. The validity of the ionic

Received: January 25, 2013

Published: March 25, 2013

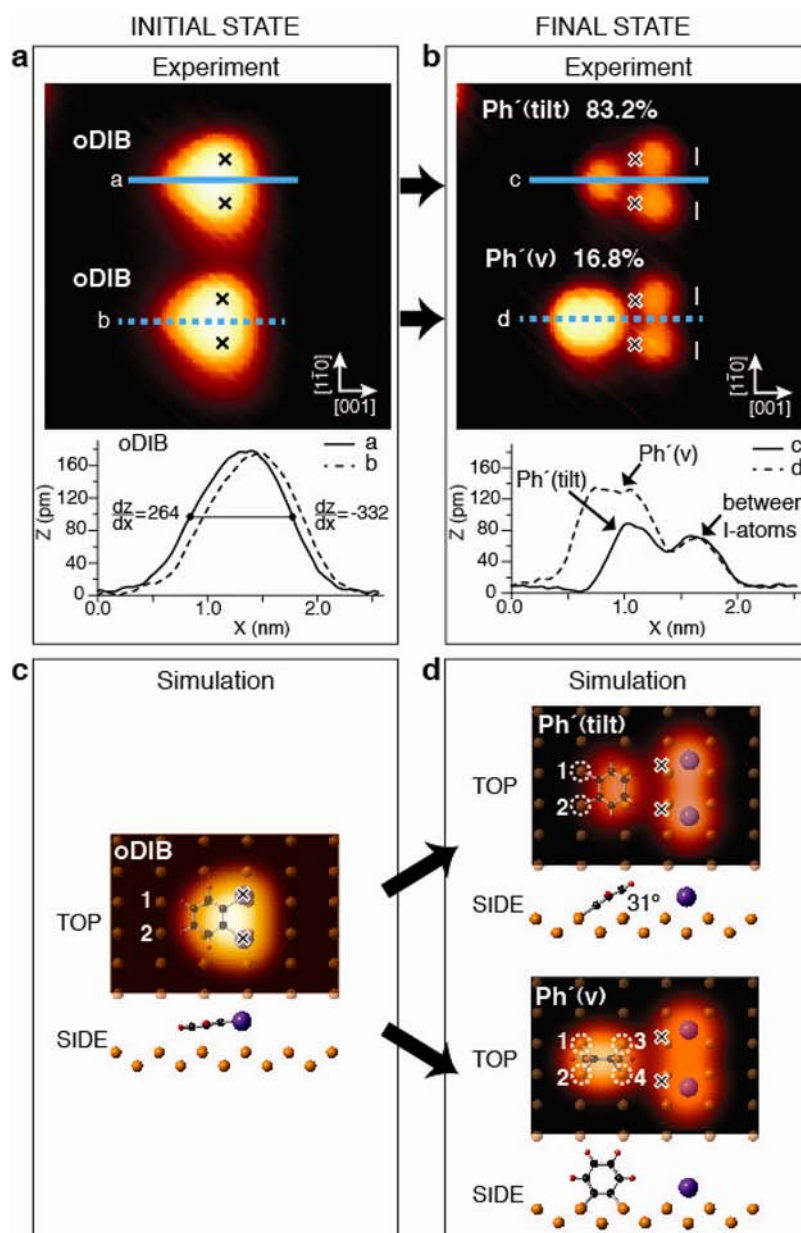


Figure 1. Experimental and simulated STM images. (a) Initial State STM image of the physisorbed reagent ortho-DIB and line profiles (a and b) bisecting the two ortho-DIB molecules along the [001] direction (the slope of the line profile is steeper at the right than at the left). (b) Final State STM image of the chemisorbed products due to electron-induced reaction at 1.1 V resulting in two C–I bonds breaking, giving two I-atoms and a phenylene (Ph') residue. Line profiles (c and d) along the [001] direction are displayed for the two product sets. Two final states were observed for phenylene, as indicated by the difference in the line profiles; c and d. Profile d shows a taller and wider protrusion than profile c. (c) Simulated image of the initial state is presented, and is in good agreement with the experiment. (d) From simulations, two final states were found for Ph', tilted and vertical, as in the experiment. Of the Ph'(tilt), one-fifth was tilted at the same angle of 31° but away from the I-atoms. The white dashed circles indicate the Cu-atoms binding to Ph', resulting in the tilted and vertical configurations. All STM images (3 × 3 nm²) were taken at 0.2 nA and +0.3 V. In all images, the crosses give the position of the I-atoms in the physisorbed ortho-DIB reagent.

pseudopotential approach^{14–16} to simulate the anionic state in this study has been tested by comparing some properties of gas phase anionic ortho-DIB calculated by the pseudopotential method and by Gaussian09 (Supporting Information Figure S3 and Tables S1 and S2).

RESULTS AND DISCUSSION

Here we show that one electron induces, almost exclusively, the reaction of two adjacent bonds in an impacted molecule at a metal surface. The system was physisorbed *o*-diiodobenzene (ortho-DIB) on Cu(110) at 4.6 K. The observed double

surface-iodination reaction was shown, by STM, to be caused by an electron of threshold energy $E_0 = 1.0$ eV. Concurrent cleavage of two neighboring C–I bonds was observed in 98% of the cases examined. It was shown experimentally that only a single-electron was required for this two-bond reaction. An “impulsive two-state” model, here termed I2S, introduced previously,^{8,9} employing DFT in VASP, predicted exclusively two-bond breaking for the present case of ortho-DIB on Cu(110). As will be shown, the I2S model gave double bond-breaking even for the extreme case that the initial impulse arose from an added electron placed wholly in a single C–I bond.

Figure 1a and b shows STM images of a pair of physisorbed ortho-DIB molecules, in the Initial State (I.S.) before and in the Final State (F.S.) after electron-induced reaction. A higher resolution STM image of the initial state is given in the Supporting Information, to show the Cu rows (Supporting Figure S1). These two molecules happened to be adjacent. When each was subjected to a pulse of ~ 0.8 nA at a voltage of 1.1 V, they gave the different F.S. outcomes shown in Figure 1b. Both yielded two I-atoms but the outcomes differed in the phenylene, Ph', which had different configurations (see below). Of the 327 cases of electron-induced reaction examined 98% ($\pm 5\%$) gave rise to two I-atoms, only 2% gave a single I-atom.

In order to characterize these STM images the I.S. and two F.S. geometries were computed by DFT and were used to generate the simulated images shown in Figure 1c and d. There is good agreement between the experimental and simulated STM images of Figure 1. In the I.S., ortho-DIB molecules physisorbed in the surface plane with the ring centered on a short-bridge site (adsorption energy, 1.3 eV), with their I-atoms to either side of [001] direction, located near short-bridge sites. In electron-induced reaction the I-atoms recoiled along the prior C–I direction to chemisorb at the nearest 4-fold hollow.

The chemisorbed organic product phenylene, Ph', is visible to the left of the pair of chemisorbed I-atoms in the F.S. image of Figure 1b. It has two distinct geometries identified by simulation: Ph'(tilt) ($83.2\% \pm 5\%$) and Ph'(v) ($16.8\% \pm 2\%$). These two geometries of Ph' are clearly distinguished in the side views of Figure 1d. For Ph'(tilt), which is the majority-pathway product, the phenylene was tilted up at 31 degrees from the surface-plane, with the two C–Cu bonds at Cu-atoms 1 and 2 in Figure 1c and d. In the case of the 'vertical' phenylene, Ph'(v), the two C–Cu bonds bridge Cu-atoms 1 and 2 at the left in Figure 1d and 3 and 4 at the right; the phenylene has its benzene ring protruding from the surface, causing its brighter appearance.

Comparing the I.S. and F.S. positions of both the I-atoms and the phenylene in Figure 1a and b, it is clear that the displacement of the products from their original position due to reaction is modest, 2.3 Å for I-atoms and 1.5 Å for phenylene (the variation in displacement was negligible). This is a further incidence of "localized atomic reaction", LAR, noted in a number of reactions at semiconductor^{2,17,18} and metal surfaces.^{6,8,9,19} The phenylene will be shown to have undergone a half-rotation.

A typical curve of the current versus time (I - t) over a physisorbed ortho-DIB near threshold bias 1.1 V, is shown in Figure 2a. The single discontinuity in the spectrum was accompanied by the formation of two chemisorbed I-atoms and the phenylene. In previous studies of electron-induced reaction,^{8,9} the I - t spectra obtained at threshold also exhibited a single discontinuity but resulted in only one chemisorbed halogen atom and an organic specie.

The number of electrons needed for the dissociation of the two C–I bonds was determined from the effect of changing current on reaction rate. The relationship between the reaction rate, R , tunneling current, I , and electron order, n , is $R \propto I^n$. The rate R is the reciprocal of the lifetime, t , of an unreacted ortho-DIB under the pulse-current conditions, taken from an exponential fit of all the observed lifetimes at each current value (for details, see Methods). A linear fit of ($\log R$) against ($\log I$), in Figure 2b gives the slope $n \approx 1$, indicating that the two C–I bonds are broken in a process involving one electron. The electron yield for this double bond-dissociation was found

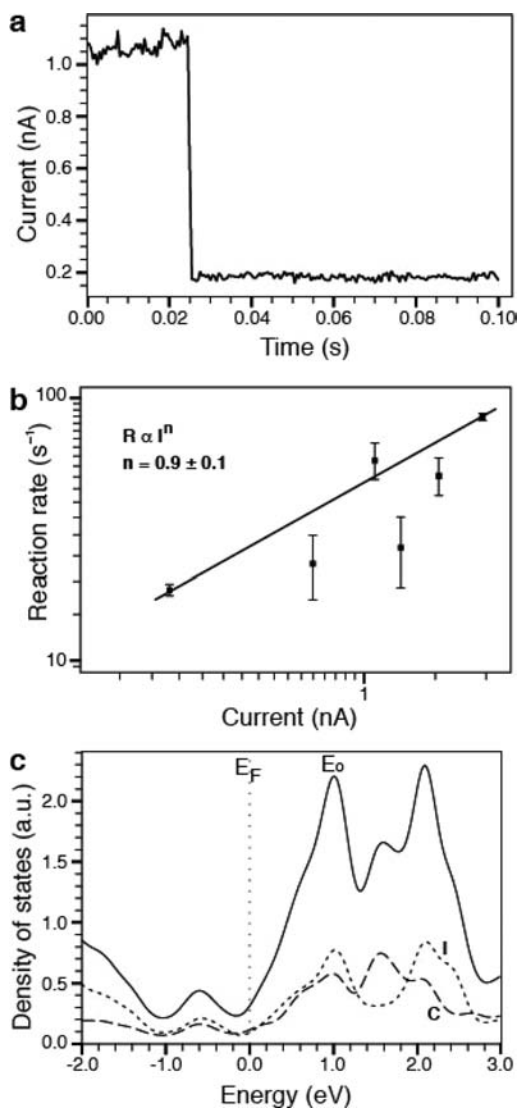


Figure 2. Electron-induced reaction of the C–I bonds of ortho-DIB at a bias of +1.1 V. (a) Current-versus-time plot showing a single downward transition which corresponds to a double C–I bond-breaking event. (b) Kinetics of the reaction, where n (0.9 ± 0.1) is the slope of the least-squares fit to the reaction rate as a function of tunneling current (log–log coordinates). Error bars are given by the error of an exponential fit (see Methods). (c) Calculated projected density of states (pDOS) of ortho-DIB on Cu(110); solid curve. The pDOS component of the I-atoms is shown by short dashes. Both the C-atom and their adjacent H-atom pDOS are shown by long dashes. E_0 refers to the energy of the lowest unoccupied molecular orbital, located at 1.0 eV.

to be $\sim 10^{-9}$, that is, $10\times$ greater than that for the single carbon–halogen bond dissociation reported previously,^{8,9} as discussed below.

The threshold energy, $E_0 \approx 1$ eV, for two-bond breaking in ortho-DIB coincided with the lowest unoccupied molecular orbital (LUMO) in our computed projected density of states for physisorbed ortho-DIB on Cu(110), shown in Figure 2c. The LUMO is the carbon–iodine, C–I, antibonding-orbital.

We have applied the previous impulsive two-state model, I2S,^{8,9} to visualize the ortho-DIB reaction-dynamics. The model uses molecular dynamics (MD) to track the progress of the physisorbed molecule for a time t^* across a repulsive antibonding anionic potential-energy state, pes^* , and thereafter

across the ground pes until the products reach their chemisorbed configuration. The time t^* is the minimum time on pes* that gives a sufficient impulse for subsequent reaction across the energy-barrier on the ground pes. In the following we placed half a unit charge on each I-atom of ortho-DIB in the antibonding anionic state, to favor two-bond breaking. The molecule needs to be propagated on pes* for only 20 fs to give sufficient impulse for subsequent reaction over the ground-state energy barrier to products. A movie of the event (Movie 1) for an initial $0.5e^-$ on each I-atom is available. (Later we will show that two-bond breaking is not dependent on this equal distribution of charge in the antibonding state, but the equal distribution yielded the major observed product configuration of phenylene, whereas $1e^-$ on a single I-atom gave a minor product configuration of phenylene, tilted as in Figure 1d but away from the I-atoms and bound to Cu-atoms 3 and 4).

Figure 3 shows five stages of the I2S computed motion across the ground pes, at intervals of several hundred femtoseconds. Figure 3a gives, from top and side, the computed initial geometry of physisorbed ortho-DIB. The copper atoms labeled 1 and 2 are those to which the phenylene formed in the reaction will ultimately bind in the F.S. of the model, in conformity with our experimental observation (see Figure 1d). At the time of Figure 3b, at 450 fs, well after the 20 fs impulse in the antibonding ionic state, the MD showed that the two I-atoms had barely begun to recoil (to the right in the figure), while the phenylene biradical had been tilted down by the force of the opposing recoil and moved to the left. At the time of 575 fs (Figure 3c) the I-atoms have both moved further to the right, but the downward force of the opposing recoil has resulted in a partial rotation of the phenylene (see Figure 3c side view) into an almost upright position. By the time of 700 fs in Figure 3d, what was previously the right-hand side of the phenylene has rotated half a turn to the left, where it is in a position to form a stretched bond with copper atoms 1 and 2. The I2S model is seen to yield only the majority observed outcome for phenylene, Ph'(tilt) (amounting experimentally to 83% of the phenylene product).

In the I2S model a total of approximately 3 ps were required on the ground pes before the pair of I-atoms came to rest, as shown in Figure 3e, chemisorbed in the nearest 4-fold hollows having recoiled a total distance of 2.3 Å from their initial positions in the physisorbed ortho-DIB. The phenylene, having rotated its pair of dangling bonds from right to left in Figure 3, is bound to copper atoms number 1 and 2 (Figure 3e). Product distributions and configurations from the I2S model are the same as those observed experimentally.

Central to this article has been the novel finding of efficient two-bond breaking due to the impact of a single electron on ortho-DIB, as against single bond-breaking for para-diodobenzene (para-DIB) and para-dichlorobenzene (para-DCB) examined previously.^{8,9} In the I2S model above, we favored the observed two-bond reaction by placing the added electron in the antibonding ionic state equally on both I-atoms of ortho-DIB. Figure 4 shows, significantly, that two C–I bond reaction is still the outcome for ortho-DIB even in the limiting case that the entire added electron was placed on a single I-atom (designated “a”). By contrast, the unequal initial-state charge distribution when applied in earlier work to para-DIB still led to single-bond breaking. This accords with the fact that the computed charge-distributions in the I2S model shown in Figure 4 give a significant charge delocalization between I-atom “a” and the nearby I-atom “b” in the case of ortho-DIB, but no

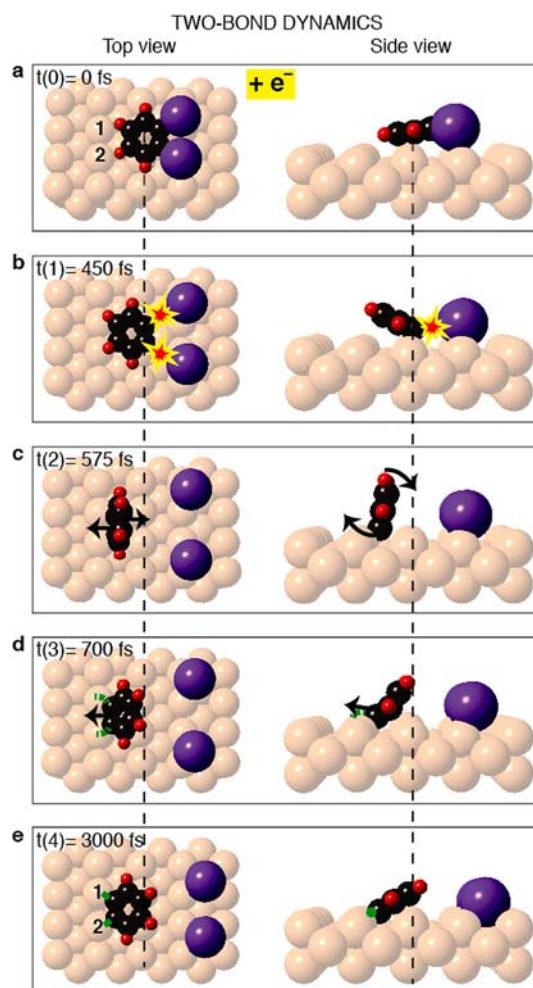


Figure 3. Molecular dynamics of the double surface halogenation for half an electronic charge on each I-atom. (a) In the initial state, the intact molecule ortho-DIB is in its most stable configuration on Cu(110). (b) After spending 20 fs in the anionic state, ortho-DIB was returned to the ground state; the impulse caused surface di-iodination, with the breaking of both C–I bonds. The two I-atoms recoiled to the right, and the phenylene, Ph', residue to the left (locus of the repulsion highlighted). (c) Phenylene performed a clockwise rotation in which the C-atom dangling bonds shifted from the right-hand side to the left. (d) Phenylene motion allowed the C-atom dangling bonds to start binding with the Cu-atoms 1 and 2. (e) Final state of the reaction is shown with the I-atoms adsorbed at nearby 4-fold hollow sites (separated by 5.1 Å), and the phenylene bound to Cu-atoms 1 and 2, tilted 31° away from the surface.

such charge delocalization between the more-widely separated I-atoms of para-DIB. Since it is this added charge entering an antibonding orbital of C–I that gives the repulsive impulse leading to reaction in the I2S model, charge delocalization between the two C–I bonds would be expected to assist two-bond reaction, as in the overwhelming majority of cases (98%) studied here.

In earlier work⁸ we showed potential-energy curves representing a computed trajectory across pes* and a minimum energy path across the ground pes. In Supporting Information Figure S2, we show a pair of such curves for para-DIB, and contrast them with pes* and pes for the present case of ortho-DIB. The most significant changes are in the greater exothermicity and the related lower activation-barrier for the ground-state pes in the case of ortho-DIB (the exothermicity

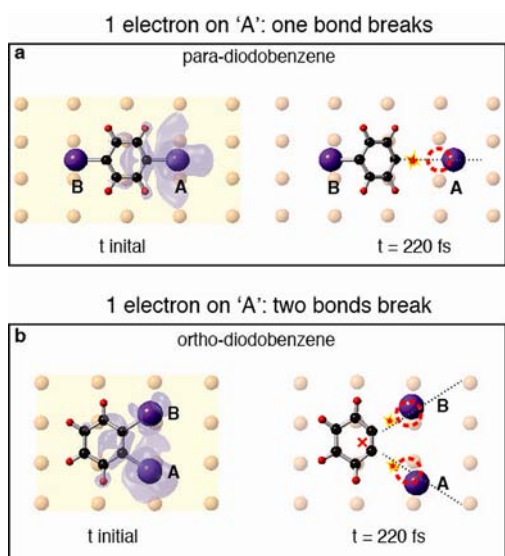


Figure 4. Comparison of reaction dynamics between para-DIB (single-bond breaking) and ortho-DIB (two-bond breaking). A full 1-electron charge was placed on I-atom “a” in each case. The configurations with yellow backgrounds denote dynamics in the anionic excited state. (a) Initial real-space distribution of the added charge for para-DIB. At $t = 0$ fs, the added charge is largely localized on the C–I bond of I-atom “a”. At $t = 220$ fs only I-atom “a” recoils away from the rest of the molecule. (b) Initial real-space distribution of added charge for ortho-DIB. At $t = 0$ fs, the added charge on ortho-DIB is spread over both C–I bonds, “a” and “b”. At $t = 220$ fs, both I-atoms recoil away from the phenylene residue of ortho-DIB.

has increased from 0.90 eV for para-DIB to 2.70 eV for ortho-DIB; the barrier height concurrently decreasing from 0.50 eV for para-DIB to 0.14 eV for ortho-DIB). The low barrier in the present case has the consequence that only a brief time, $t^* = 20$ fs, on the ionic state (cf. $t^* = 80$ fs for para-DIB⁸) suffices to distort and accelerate the molecule sufficiently for it to surmount the ortho-DIB ground-state barrier. The short ionic residence time of 20 fs is in qualitative accord with the observed high yield (10^{-9} for ortho-DIB compared to 10^{-10} for para-DIB⁸), on the basis of Gadzuk’s²⁰ postulate of exponential decay in probability for ionic adsorbates over time.

CONCLUSION

The observed highly efficient concerted breaking of the two C–I bonds of ortho-DIB is ascribed primarily to the delocalization of charge from one I-atom to the closely neighboring one by way of overlapping antibonding orbitals. Since the experiments only yield information regarding the initial and final states, we cannot say whether the concerted bond-breaking following single-electron excitation is “simultaneous” or “consecutive”.²¹ This is a question we hope will be addressed by others employing femtosecond time-resolved measurement.

There is currently widespread interest in the electron-induced reaction of physisorbed molecules. These studies, performed here and elsewhere at semiconductor and metal surfaces, have shown that one low-energy electron incident on the adsorbate induces the severance of a single bond. Here we show experimentally, for electron-induced reaction in ortho-diodobenzene, efficient two-bond breaking, which theory, also reported here, ascribes to the *intramolecular* delocalization of the added single-electron charge. In a recent related study,⁵ we gave evidence of the comparable effect of *intermolecular* charge

delocalization of a single electron leading to efficient multiple bond-breaking. In that case, as in the present one, we ascribe the charge delocalization to overlap between adjacent antibonding orbitals in which the added electron was placed. (Our earlier studies of electron-induced reaction in para-diodobenzene showed only local single-bond reaction, in the absence of antibonding overlap.^{8,9}) Nature may employ similar means of charge delocalization to enhance the efficiency of photoreaction, by channeling photoproduced electrons through overlapping antibonding orbitals to multiple reaction sites.

ASSOCIATED CONTENT

Supporting Information

A figure showing a higher resolution STM image of the initial state, the minimum energy pathways for para- and ortho-DIB bond-breaking reactions, theoretical calculations of anionic models in the pseudopotential method and Gaussian09 for molecular orbitals, C–I bond-length, and energy gaps. This material is available free of charge via the Internet at <http://pubs.acs.org>.

Web-Enhanced Feature

A movie of the two-state model is available in the HTML version of the paper.

AUTHOR INFORMATION

Corresponding Author

jpolanyi@chem.utoronto.ca

Present Address

†K.H.: Department of Chemical Physics, Fritz-Haber-Institut der Max-Planck-Gesellschaft, Faradayweg 4–6, D-14195 Berlin, Germany.

Notes

The authors declare no competing financial interest.

ACKNOWLEDGMENTS

This work was funded in part by the Natural Sciences and Engineering Research Council of Canada (NSERC) and Xerox Research Centre Canada (XRCC). We are grateful to Professors Hong Guo and Wei Ji for many helpful discussions. Computations were performed on TCS at SciNet HPC Consortium funded by the Canada Foundation for Innovation.

REFERENCES

- Avouris, Ph.; Wolkow, R. *Phys. Rev. B* **1989**, *39*, 5091–5100.
- McNab, I. R.; Polanyi, J. C. Imprinting Atomic and Molecular Patterns. In *Frontiers of Nanoscience, Atomic and Molecular Manipulation*; Mayne, A. J., Dujardin, G., Eds.; Elsevier: Amsterdam, 2011; Vol. 2, pp 79–120.
- Hla, S. W.; Meyer, G.; Rieder, K. H. *ChemPhysChem* **2001**, *2*, 361–366.
- Ho, W. J. *Chem. Phys.* **2002**, *117*, 11033–11061.
- Ning, Z.; Polanyi, J. C. *Angew. Chem., Int. Ed.* **2013**, *52*, 320–324.
- Maksymovych, P.; Sorescu, S. D.; Jordan, K. D.; Yates, J. T., Jr. *Science* **2008**, *322*, 1664–1667.
- Horcas, I.; Fernández, R.; Gómez-Rodríguez, J. M.; Colchero, J.; Gómez-Herrero, J.; Baro, A. M. *Rev. Sci. Instrum.* **2007**, *78*, 013705.
- Leung, L.; Lim, T.; Ning, Z.; Polanyi, J. C. *J. Am. Chem. Soc.* **2012**, *134*, 9320–9326.
- Eisenstein, A.; Leung, L.; Lim, T.; Ning, Z.; Polanyi, J. C. *Faraday Disc.* **2012**, *157*, 337–353.
- Kresse, G.; Furthmüller, J. *Phys. Rev. B* **1996**, *54*, 11169–11186.
- Grimme, S. J. *Comput. Chem.* **2004**, *25*, 1463–1475.

- (12) Perdew, J. P.; Ernzerhof, M.; Burke, K. *J. Chem. Phys.* **1996**, *105*, 9982–9985.
- (13) Palotás, K.; Hofer, W. A. *J. Phys.: Condens. Matter* **2005**, *17*, 2705–2713.
- (14) Kresse, G.; Joubert, D. *Phys. Rev. B* **1999**, *59*, 1758–1775.
- (15) Ji, W.; Lu, Z. Y.; Gao, H. *Phys. Rev. Lett.* **2006**, *97*, 246101.
- (16) Köhler, L.; Kresse, G. *Phys. Rev. B* **2004**, *70*, 165405.
- (17) Guo, H.; Ji, W.; Polanyi, J. C.; Yang, J. *ACS Nano* **2008**, *2*, 699–706.
- (18) Harikumar, K. R.; McNab, I. R.; Polanyi, J. C.; Zabet-Khosousi, A.; Hofer, W. A. *Proc. Natl. Acad. Sci. U.S.A.* **2011**, *108*, 950–955.
- (19) Ning, Z.; Polanyi, J. C. *J. Chem. Phys.* **2012**, *137*, 091706.
- (20) Gadzuk, J. W. *Phys. Rev. B* **1991**, *44*, 13466.
- (21) Liu, R.; Cui, Q.; Dunn, K. M.; Morokuma, K. *J. Chem. Phys.* **1996**, *105*, 2333–2345.